Title

COMPARISON OF LASER-INDUCED FLUORESCENCE AND SCATTERING IN POOL-FIRE DIFFUSION FLAMES

Authors

Bard, S.
Pagni, P.J.

Publication Date

1980-09-01

LBL-12768
Preprint c.2

Lawrence Berkeley Laboratory
UNIVERSITY OF CALIFORNIA

ENERGY & ENVIRONMENT
DIVISION

Submitted to the Journal of Quantitative Spectroscopy
and Radiative Transfer

COMPARISON OF LASER-INDUCED FLUORESCENCE AND SCATTERING IN POOL-FIRE DIFFUSION FLAMES

S. Bard and P.J. Pagni

September 1980

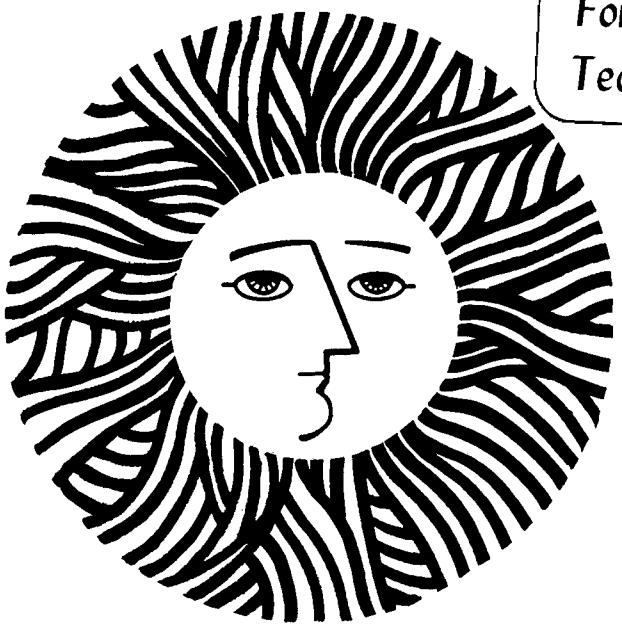

Prepared for the U.S. Department of Energy under Contract W-7405-ENG-48

DISCLAIMER

COMPARISON OF LASER-INDUCED FLUORESCENCE AND SCATTERING IN POOL-FIRE DIFFUSION FLAMES[+]

S. Bard[‡] and P.J. Pagni

Mechanical Engineering Department

and

Lawrence Berkeley Laboratory

University of California

Berkeley, CA 94720

September 1980

To be published in the Journal of Quantitative Spectroscopy and Radiative Transfer

[+]This work was supported by the Center for Fire Research of the National Bureau of Standards, of the U.S.D.O.C. under Grant No. NB 80 NAG-E6839 which was administered by the U.S. Department of Energy under Contract No. W-7405-ENG-48.

The assistance of Factory Mutual Research Corporation and Dr. C. Chan is appreciated.

[‡] Current address: Jet Propulsion Laboratory, Mail Stop 157-102, 4800 Oakgrove Dr., Pasadena, CA 91103

ABSTRACT

Measurements of fluorescence and scattering in small-scale, 0 (10 cm diameter), buoyant diffusion flames indicate that absorption of visible laser radiation by gaseous molecules or radicals is negligible compared to absorption and scattering by carbon particulates. Previous experiments determined soot volume fractions and particulate-size distributions in similar polystyrene and polymethylmethacrylate flames by attributing visible laser extinction measurements entirely to carbon particles. Those results are, therefore, not affected by the error in neglecting gas-species absorption. The fluorescence spectra presented here are similar to diffusion flame results in the literature.

Introduction

Light extinction is usually attributed entirely to carbon particles in experiments which derive particulate characteristics from light transmission or scattering measurements.[1-4] However, large-molecule gaseous soot precursors and unburned pyrolozate may contribute to extinction of the laser beam.[5-10] It is anticipated that this absorption would have more relative significance in regions without much soot, such as the small zone between the pyrolyzing fuel surface and the luminous flame. Indeed, several authors[5-8] have found evidence of absorption by what are probably polycyclic aromatic hydrocarbon (PAH) molecules or radicals in the pyrolysis region of diffusion flames and near the reaction zone of premixed flames. Laser-induced fluorescence measurements, at the same visible laser wavelengths as used in extinction experiments indicate that this gaseous absorption is less for diffusion flames than for premixed flames.

All of the soot volume fraction measurements reported previously[1-4] for pool fires were done at heights within the flame where much soot was present, at least 2 cm above the fuel surface. If absorbing gaseous species also exist in these regions of the flames and are neglected in determining particulate volume fractions and size distributions, then overestimates may result. If, however, these gaseous species absorp less than ~1% of the incident laser intensity, then the errors introduced would only be of the order of the accuracy of the detectors and therefore negligible. The following experiment was designed to estimate the fraction of the incident laser intensity which is absorbed by gas-phase molecules or radicals from fluorescence measurements taken at the same

flame size and laser location as the previously reported extinction measurements[1-4] for polystyrene (PS) and polymethylmethacrylate (PMMA).

Extinction Analysis

Consider a monochromatic beam of radiation incident on a cloud of soot particles and absorbing gas. Let I_o be the incident intensity, I be the transmitted intensity and I_i be the intensity attenuated by the i^{th} phenomenon; then

$$I_o = I + \sum_i I_i \quad , \quad i = a, s \text{ and } g \tag{1}$$

where the subscripts indicate particulate absorption and scattering, and gaseous absorption, respectively. A total extinction coefficient, τ, may be defined by

$$I/I_o = \exp(-\tau L) \tag{2}$$

where L is pathlength through the cloud and all attenuating phenomenon are incorporated, i.e., $\tau = \sum_i \tau_i$, $i = a, s$ and g. Then each attenuator contributes

$$I_i/I_o = [1 = \exp(-\tau L)]\ \tau_i/\tau \quad , \quad i = a, s \text{ and } g \tag{3}$$

to the total extinction. The particulate extinction coefficients can be evaluated from

$$\tau_i = \int_0^\infty N(r)\ Q_i\ (\lambda, m, r)\pi r^2 dr \quad , \ i = a \text{ and } s \tag{4}$$

where Q_a and Q_s may be obtained from the Mie scattering theory.[11] The size distribution used here was a Gamma distribution with $\sigma/r_m = 1/2$, i.e.,

$$N(r)dr = N_o\ (27\ r^3/2r_{max}^4)\ \exp(-3r/r_{max})\ dr \tag{5}$$

where N_o is the particle concentration and r_{max} is the most probable

particle radius. From Eq. (3)

$$\frac{I_g}{I_o} = \frac{[1 - \exp(-\tau L)]\, I_g/I_s}{1 + \tau_a/\tau_s + I_g/I_s} \quad . \tag{6}$$

This equation may be used to determine the fraction of the incident energy absorbed by gas-phase species. As a first approximation, τ_a and τ_s are given by Eq. (4), using the experimental size distributions given in Ref. 2 for the limiting cases considered here of a very sooty flame, $f_v = 3.3 \times 10^{-6}$ for PS and a relatively clean flame, $f_v = 2.2 \times 10^{-7}$ for PMMA. The measured extinction coefficients, τ, have also been reported in Ref. 2 and only I_g/I_s remains unknown on the right-hand side of Eq. (6). The following experiment is designed to estimate I_g/I_s from the measured ratio of the laser-induced fluorescence intensity to the scattering intensity.

Experiment

Figure 1 shows an apparatus schematic. The measurements were taken at right angles to the laser beam direction. A CW Coherent (model CR-MG) argon/krypton ion laser operating at λ = 488 nm and with an output of ~250 mW was used as the light source. The originally vertically polarized beam (quality > 100:1) was rotated to the horizontal with a Newport Research Beam Steering Instrument (model BSD-1) and a Hoya PL 67 polarizing filter was used to eliminate any stray vertical polarization. An f = 147 mm lens focused the scattered radiation at θ = 90° onto the entrance slit of a 250 mm focal length Jarrell-Ash (model 82-410) monochromator. The entrance slitwidth of 0.1 mm was blocked off to a height of 1 mm, which was the diameter of the beam image. The monochromator bandwidth was 0.3 nm.

The light leaving the exit slit was focused onto an RCA 1P28 photomultiplier tube mounted in a Pacific Photometric 3377D housing and run at 1000 V. The laser beam was chopped with an Ithaco (model 383A) variable-speed chopper run at a frequency of 500 Hz. An output reference signal from the chopper was input to an Ithaco (model 395) lock-in amplifier along with the photomultiplier signal. This phase-sensitive detection is a standard procedure to eliminate any flame emission.

The fuels combusted were polystyrene and polymethylmethacrylate beads in a 7.5 cm diameter, 1 cm high dish. The beam height was 2 cm above the fuel surface, with the probe volume directly above the center of the dish. Each fuel was allowed to burn for $\lesssim$ 10 min during which time the fuel regressed only ~2 mm below the rim of the dish. The dish was then refilled with fuel and reignited. This procedure was repeated until measurements were recorded over the desired wavelength range. The wavelength scale of the monochromator was scanned from 400 to 600 nm at 10 nm intervals. Near the laser wavelength, the scanning interval was decreased to 0 (1 nm) to determine any fine detail of the spectra.

Spectra

The resulting spectra for both fuels are shown in Figs. 2 and 3. The ordinate units of current are actually arbitrary, since all that is required to solve Eq. (6) is the ratio of gaseous absorption to particulate scattering. This ratio makes it unnecessary to obtain absolute scattered power through a difficult evaluation of all view factors and optical losses. The shapes of the fluorescence spectra are similar for both fuels and closely resemble those found in the literature.[5-8] A

major difference here is the large amount of particulate scattering found at the laser wavelength. The lack of a resolved band structure suggests that the fluorescence originates from large polyatomic molecules, probably polycyclic aromatic hydrocarbons with $O(3\text{-}10)$ benzene rings,[5-7] which would be expected to absorb in the visible. Polycyclic aromatic radicals or polyacetylenic radicals are also possibilities.[5-7] Both Stokes (emission at longer wavelengths than the excitation) and anti-Stokes (emission at shorter wavelengths than the laser) fluorescence are present, with slightly more of the former. There appears to be a similar set of absorbing species in pool fires, counterflow diffusion flames and premixed flames.

The key measurement here, the ratio of the energy in the fluorescence to that scattered, is obtained graphically from the respective areas under spectra. Near the laser line, the portion of the scattering spectrum above the fluorescence region was considered as scattered energy and the area below as fluorescence. For PS (Fig. 2), the area ratios yield $i_f/i_s = 0.045$. For PMMA (Fig. 3) $i_f/i_s = 0.16$.

Some of the energy absorbed by the gaseous molecules is dissipated by molecular collisions. The remainder is reemitted by fluorescence. A fluorescence efficiency may be defined as the ratio of the total fluorescent energy radiated to the energy absorbed by these species, viz,

$$\eta_f = I_f/I_g \quad . \tag{7}$$

Typical fluorescence efficiencies for ethylene-oxygen flames have been estimated[5] at $\eta_f \sim 0.1$ for premixed flames, and $\eta_f \sim 0.05$ for counterflow diffusion flames. However, it is suggested[5] that this latter value be doubled because of the high uncertainty due to a total beam attenuation

of only 1%. Haynes and Wagner[8] measured fluorescence efficiencies of $O(10^{-2})$ in ethylene-air flames. Di Lorenzo et al[7] observed $10^{-2} \lesssim \eta_f \lesssim 10^{-1}$ when the soot in their rich methane-oxygen premixed flames is taken into account. The fluorescence efficiency is assumed to be in that range in the following analysis.

Scattering Analysis

The spectra in Figs. 2 and 3 were taken at $\theta = 90°$. The total scattering and fluorescence in all directions will now be interpolated from Mie scattering theory to evaluate I_g/I_s from those spectra.

Consider a laser beam of intensity I_o incident on a scattering particle. Let the scattered intensity in the direction θ,ϕ be represented by $i(\theta,\phi)$. The angle of observation, θ, is measured from the forward to the scattered direction in the plane defined by the forward and scattered directions. The angle of this observation plane with respect to the vertical is the azimuthal angle, ϕ. The total scattering into the sphere of 4π steradians is defined by the integral of i over all directions,

$$I_s = \int_{4\pi} i_s(\theta,\phi)\, d\Omega_s \quad . \tag{8}$$

If the scattering is isotropic, then $i_s = I_s/4\pi$. A phase function, $p(\theta,\phi)$, can be defined[12] as the ratio of the intensity scattered in the direction θ,ϕ to that scattered by an isotropic scatterer,

$$p(\theta,\phi) = i_s\,(\theta,\phi)\; 4\pi/I_s \quad . \tag{9}$$

Carbon particles 2 cm above the fuel surface in a buoyant diffusion flame are young enough that their shape is approximately spherical[13] and yet

old enough that their optical properties[14] are well characterized, i.e., for $\lambda = 488$ nm, $m = 1.94 - 0.54i$.

The phase function may be obtained under these assumptions from the Mie scattering theory in terms of scattering functions, $i_\perp$ and $i_{||}$, polarized perpendicular and parallel, respectively, to the observation plane,

$$p(\theta) = 2[i_\perp(\theta) + i_{||}(\theta)]/(Q_s \alpha^2) \quad , \tag{10}$$

where

$$i_\perp = \sum_{n=1}^{\infty} \frac{2n+1}{n(n+1)} (a_n \pi_n + b_n \gamma_n) \tag{11a}$$

and

$$i_{||} = \sum_{n=1}^{\infty} \frac{2n+1}{n(n+1)} (a_n \gamma_n + b_n \pi_n) \quad ; \tag{11b}$$

π_n and γ_n are the angular functions derived from the Legendre polynomials

$$\pi_n (\cos\theta) = dP_n (\cos\theta)/d(\cos\theta) \tag{12a}$$

and

$$\gamma_n (\cos\theta) = \cos\theta \, \pi_n (\cos\theta) - \sin^2\theta \, d\pi_n(\cos\theta)/d\cos\theta \quad . \tag{12b}$$

where the Legendre polynomials are defined by

$$P_n(x) = \frac{1}{2^n n!} \frac{d^n(x^2 - 1)}{dx^n} \quad , \tag{13}$$

and the scattering is independent of ϕ.

Figure 4 shows the phase functions for incident radiation polarized perpendicular and parallel to the observation plane, along with their sum (which is equivalent to unpolarized incident radiation) for monodisperse particle size distributions at various $\alpha = 2\pi r/\lambda$. Figure 4a describes Rayleigh scattering ($\alpha << 1$). The incident energy polarized perpendicular to the observation plane is scattered uniformly while the

energy polarized parallel to the observation plane is zero at $\theta = 90°$ and is symmetrical about that scattering angle. As α increases in Figs. 4b and 4c, forward scattering becomes dominant, while the parallel phase function magnitude at $\theta = 90°$ remains small.

The phase functions in Fig. 4b well represent all the flame particulate measured in Ref. 2. Since 20 nm < r_{max} < 65 nm, the range of most probable optical size parameters using common visible lasers (457.9 nm to 632.8 nm) is $0.2 < \alpha_{max} < 0.9$. Figures 4a and 4c represent uncommon limiting cases. If scattering techniques are used to determine particle volume fractions or sizes,[8,15-17] measurement at a forward angle, e.g., $\theta \sim 40°$, with the laser polarity perpendicular to the observation plane would minimize fluorescence interference. However, because of low scattered signal levels, quantitative corrections for fluorescence may still be necessary. Multiple wavelength transmission experiments for particle volume fractions and size distributions have the least fluorescence interference. Here, the laser beam has been polarized in the observation plane and measurements made at $\theta = 90°$ to minimize detection of particulate scattering and emphasize fluorescence.

In contrast to the scattering, the fluorescence will be isotropic and unpolarized. Therefore, the ratio of the intensity absorbed by gas species to that scattered by particulates, in terms of the measured fluorescence intensity, i_f, and scattering intensity, i_s, is

$$I_g/I_s = [i_f(\theta=90°)/i_s\ (\theta=90°)][p\ (\theta=90°)/\eta_f] \quad . \qquad (14)$$

Any attenuation of the measured i's by particulate present between the probe volume and the detector cancels.

Results

Table 1 lists the two i_f/i_s measured from Figs. 2 and 3 and the calculations using those measurements in Eqs. (14 and 6) for the gas absorbed intensity as a fraction of the scattered and incident intensities respectively. The extinction coefficients and ratios of absorption to scattering coefficients were determined from Eq. (4) using the size distributions measured in Ref. 2 for polystyrene and polymethylmethacrylate. The phase functions were calculated for a single particle at the most probable radii for these fuels with the angle of observation at $\theta = 90°$ and the incident laser beam polarized parallel to the observation plane. The beam pathlength was taken as L = 7.0 cm.

A reasonable range of fluorescence efficiencies, as shown, was obtained from the literature;[5-8] none were measured here. This range yields gas-absorbed intensities from 0.07 to 2 percent of the particle scattering intensities. However, particles with the size distribution parameters[2] listed and the optical properties[14] cited previously absorb even more than they scatter, so that the gas-absorbed intensities are even smaller fractions of the incident intensities, from 0.03 to 0.7 percent of I_o. The total attenuation is typically O (50) percent of I_o and the detector accuracy is of O (1) percent of I_o. Thus, the fluorescence effects are shown to be negligible for both a very sooty flame (PS) and a clean one (PMMA). This is probably due to prohibition, by the turbulent structure within these buoyant diffusion flames, of significant regions where the PAH concentration dominates the soot concentration.

The results justify using the N(r) from Ref. 2 and no iteration is necessary. I_g/I_o increases weakly with L until the optically thick condition ($\tau L >> 1$) is reached as indicated by Eq. (6). PS is already thick at L = 7 cm. For PMMA, I_g/I_o will increase by 20% when its flames become thick at L ~ 1 m. In the thick limit, $I_g/I_o \approx 8.5 \times 10^{-3}$ for PMMA which is still < 1% and the neglect of fluorescence is permissible for all flame sizes.

While measurements of i_f/i_s were only made at 488 nm, similar literature measurements[6-8] of fluorescence spectra at 457.9, 488.0, 514.5 and 632.8 nm indicate fluorescence intensities slowly decrease as the incident wavelength increases. Since the short wavelength end of the visible region is used here, conclusions based on the magnitudes of I_g/I_s and I_g/I_o in Table 1 may be extended to all visible incident wavelengths.

The neglect of fluorescence is also supported by the consensus obtained among several investigators[1-4,8,16-18] using different techniques to measure soot volume fractions, f_v, and size distributions in diffusion flames of a wide variety of fuels. Greater variation exists within a given flame or among differently fueled flames than among investigators examining similar systems. The following magnitudes cover all available local observations: $10^{-8} \lesssim f_v \lesssim 10^{-5}$, 10 nm $\lesssim r_{max} \lesssim 10^2$ nm, and 10^6 cm$^{-3} \lesssim N_o \lesssim 10^{12}$ cm^{-3}.

Conclusions

Fluorescence measurements in PS and PMMA pool fires confirm that there are other species besides carbon particulate which attenuate visible laser radiation. However, these gas-phase species have been shown

to absorb less than the limit of accuracy, i.e., 1% of the incident laser power, of the detectors used in multiwavelength transmission experiments previously reported.[1-4] It may, therefore, be assumed that only soot-particle absorption and scattering occur in determining particulate volume fractions and size distributions using this method.

It has been demonstrated that fluorescence has no significant effect on in-situ multiwavelength transmission measurements of diffusion flame carbon particulate size distributions.

ACKNOWLEDGEMENT

This work was supported by the Center for Fire Research of the National Bureau of Standards of the U. S. D.O.C. under Grant No. NB 80 NAG-E6839 which was administered by the U.S. Department of Energy under Contract No. W-7405-ENG-48.

REFERENCES

1. P.J. Pagni and S. Bard, "Particulate Volume Fractions in Diffusion Flames," Seventeenth Symposium (International) on Combustion, pp. 1017-1028, The Combustion Institute, Pittsburgh, PA (1978).

2. S. Bard and P.J. Pagni, "Carbon Particulate in Small Pool-Fire Flames," A.S.M.E. J. Heat Transfer, in press.

3. S. Bard and P.J. Pagni, "Spatial Variation of Soot Volume Fractions in Pool-Fire Diffusion Flames," Comb. and Flame, in press.

4. S. Bard, "Diffusion Flame Particulate Volume Fractions," Ph.D. Dissertation, Mechanical Engineering Dept., University of California, Berkeley (1980).

5. K. Muller-Dethlefs, "Optical Studies of Soot Formation and the Addition of Organic Peroxides to Flames," Ph.D. Dissertation, Dept. of Chemical Engineering and Chemical Technology, Imperial College, London (1979).

6. G.W. Mallard, P.K. Schenck and K.C. Smyth, Center for Fire Research, National Bureau of Standards, private communication (1979).

7. A. Di Lorenzo, A. D'Alessio, V. Cincotti, S. Masi, P. Menna and C. Venitozzi, "UV Absorption, Laser-Excited Fluorescence and Direct Sampling in the Study of Formation of Polycyclic Aromatic Hydrocarbons in Rich CH_4/O_2 Flames," Eighteenth Symposium (International) on Combustion, The Combustion Institute, Pittsburgh, PA, in press.

8. B.S. Haynes and H. Gg. Wagner, Ber. Bunsenges. Phys. Chem. 84, 499 and 585 (1980).

9. B.L. Wersborg, L.K. Fox and J.B. Howard, Comb. and Flame 24, 1 (1975).

10. T. Kashiwagi, Comb. Sci. and Tech. 21, 131 (1980).

11. G. Mie, Ann. Physik, Ser. 4, 25, 377 (1908).

12. H.C. Hottel and A.F. Sarofim, Radiative Transfer, McGraw-Hill, New York, N.Y. (1967).

13. B.L. Wersborg, J.B. Howard and G.C. Williams, "Physical Mechanisms in Carbon Formation in Flames," Fourteenth Symposium (International) on Combustion, pp. 929-940, The Combustion Institute, Pittsburgh, PA (1973).

14. S-C. Lee and C-L. Tien, "Optical Constants of Soot in Hydrocarbon Flames," Eighteenth Symposium (International) on Combustion, The Combustion Institute, Pittsburgh, PA, in press.

15. A. D'Allessio, A. Di Lorenzo, A. Borghese, F. Baretta and S. Masi, "Study of the Soot Nucleation Zone of Rich Methane-Oxygen Flames," Sixteenth Symposium (International) on Combustion, pp. 695-708, The Combustion Institute, Pittsburg, PA (1976).

16. J.H. Kent, H. Jander and H. Gg. Wagner,"Soot Formation in a Laminar Diffusion Flame," Eighteenth Symposium (International) on Combustion, The Combustion Institute, Pittsburgh, PA, in press.

17. I. J. Jagoda, G. Prado and J. Lahaye, Comb. and Flame 37, 261 (1980).

18. M. Kunugi and H. Jinno, "Determination of Size and Concentration of Soot Particles in Diffusion Flames by a Light-Scattering Technique," Eleventh Symposium (International) on Combustion, pp. 257-266, The Combustion Institute, Pittsburgh, PA (1967).

NOMENCLATURE

a_n	$\dfrac{\psi_n(\alpha)\psi_n'(\beta) - m\,\psi_n(\beta)\psi_n'(\alpha)}{\zeta_n(\alpha)\psi_n'(\beta) - m\,\psi_n(\beta)\zeta_n'(\alpha)}$
b_n	$\dfrac{m\,\psi_n(\alpha)\psi_n'(\beta) - \psi_n(\beta)\psi_n'(\alpha)}{m\,\zeta_n(\alpha)\psi_n'(\beta) - \psi_n(\beta)\zeta_n'(\alpha)}$
f_v	soot volume fraction
I	radiant intensity
$i(\theta,\phi)$	radiant intensity in direction θ,ϕ
L	pathlength
m	complex index of refraction
n	real index of refraction
nk	imaginary index of refraction
N(r)dr	particle concentration in the size range dr about r
N_o	total particle concentration
p	ratio of intensity scattered into direction θ,ϕ to that scattered by an isotropic scatterer
r	particle radius

Greek Symbols

α	$2\pi r/\lambda$
β	$m\alpha$
$\zeta_n(z)$	$\left(\frac{\pi z}{2}\right)^{1/2} H^{(2)}_{n+1/2}(z)$, where $H^{(2)}_{n+1/2}(z)$ are the half integer order Hankel functions of second kind
η_f	fluorescence efficiency, I_f/I_g
θ	angle of observation in the plane defined by the forward and observed directions

λ	wavelength
τ	extinction coefficient
ϕ	angle of observation plane with the vertical
$\psi_n(z)$	$\left[\frac{\pi z}{2}\right]^{1/2} J_{n+1/2}(z)$, where $J_{n+1/2}(z)$ are the half integer order Bessel functions of first kind

Subscripts

a	absorption by particulate
f	fluorescence
g	gaseous
m	mean
max	most probable, i.e., at maximum in N(r)
o	incident
s	scattering
	polarized in observation plane
	polarized normal to observation plane

TABLE CAPTION

Table 1. Summary of the intensity absorbed by gas-phase fluorescing species as fractions of the particulate scattered intensity and the incident intensity.

Table 1

	POLYSTYRENE	POLYMETHYLMETHACRYLATE
Measured ratio of fluorescence to parallel scattering at $\theta = 90°$, i_f/i_s	0.045	0.16
Most probable radius, r_{max}, nm	47	45
Parallel phase function, $p(\theta = 90°)$	1.6×10^{-3}	1.3×10^{-3}
Estimated fluorescence efficiency, η_f	$10^{-1} - 10^{-2}$	$10^{-1} - 10^{-2}$
Ratio of gas absorbed intensity to particle scattered intensity, I_g/I_s	$7 \times 10^{-4} - 7 \times 10^{-3}$	$2 \times 10^{-3} - 2 \times 10^{-2}$
Particle concentration, N_o, cm^{-3}	1.7×10^{9}	1.3×10^{8}
Extinction coefficient calculated for N(r) measured in Ref. 2, τ, cm^{-1}	0.55	0.035
Ratio of absorption to scattering coefficients for same N(r) as τ, τ_a/τ_s	1.3	1.3
Fraction of incident intensity absorbed by fluorescing gas, I_g/I_o	$3 \times 10^{-4} - 3 \times 10^{-3}$	$7 \times 10^{-4} - 7 \times 10^{-3}$

FIGURE CAPTIONS

1. Schematic of apparatus used for laser-induced fluorescence and scattering measurements.
2. Fluorescence and scattering spectra measured on the centerline of a polystyrene diffusion flame 2 cm above the 7.5 cm diameter fuel surface.
3. Fluorescence and scattering spectra measured on the centerline of a polymethylmethacrylate diffusion flame 2 cm above the 7.5 cm diameter fuel surface.
4. Scattering phase function versus scattering angle with $m = 1.95 - 0.54\,i$ for three particle size parameters: a) $\alpha \ll 1$, b) $\alpha = 0.65$ and c) $\alpha = 2.6$. The symbols ($\perp$) and ($\parallel$) refer to incident energy polarized perpendicular and parallel, respectively, to the plane of observation, and (U) is their sum which applies for unpolarized incident radiation.

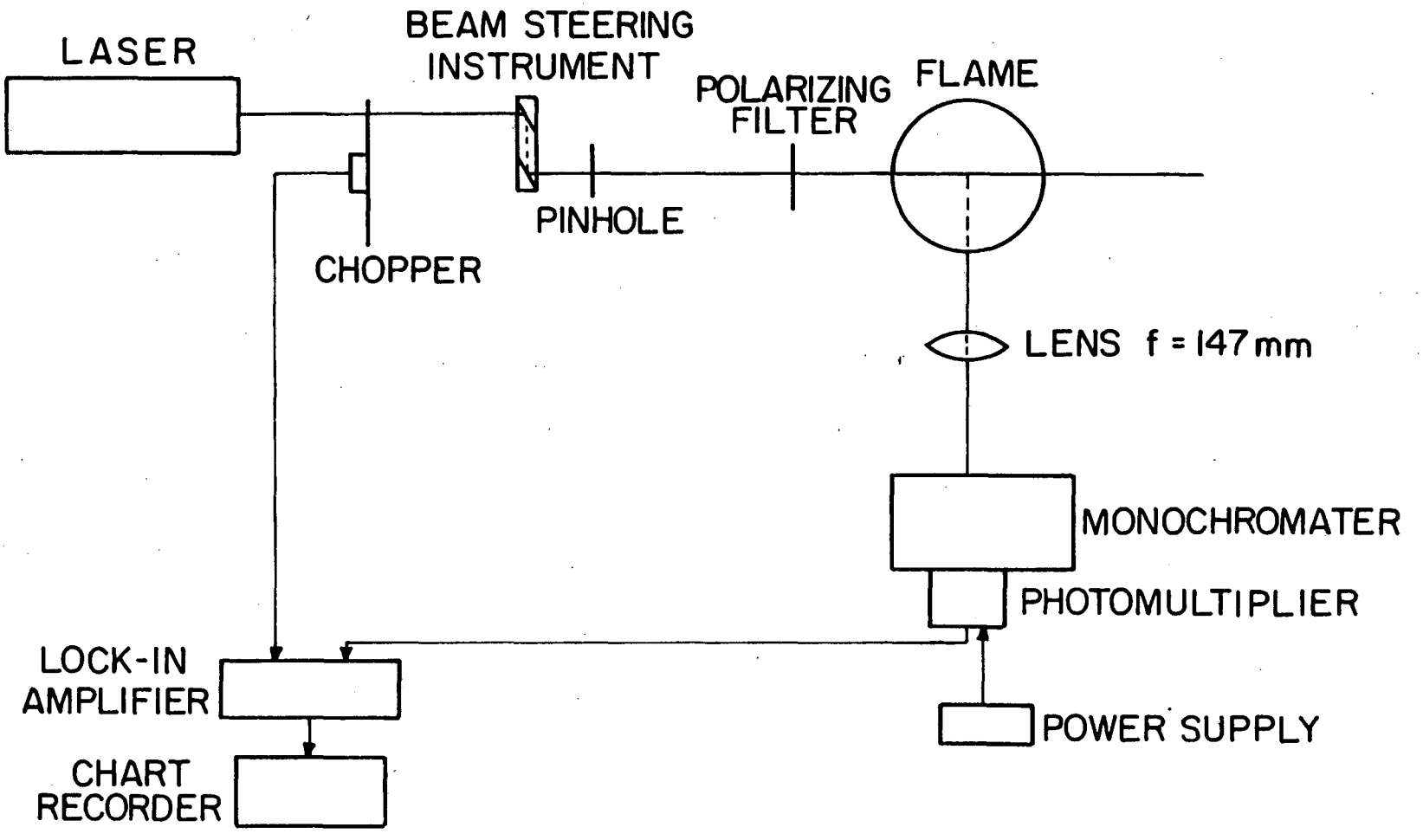

Fig. 1

XBL 805-5146

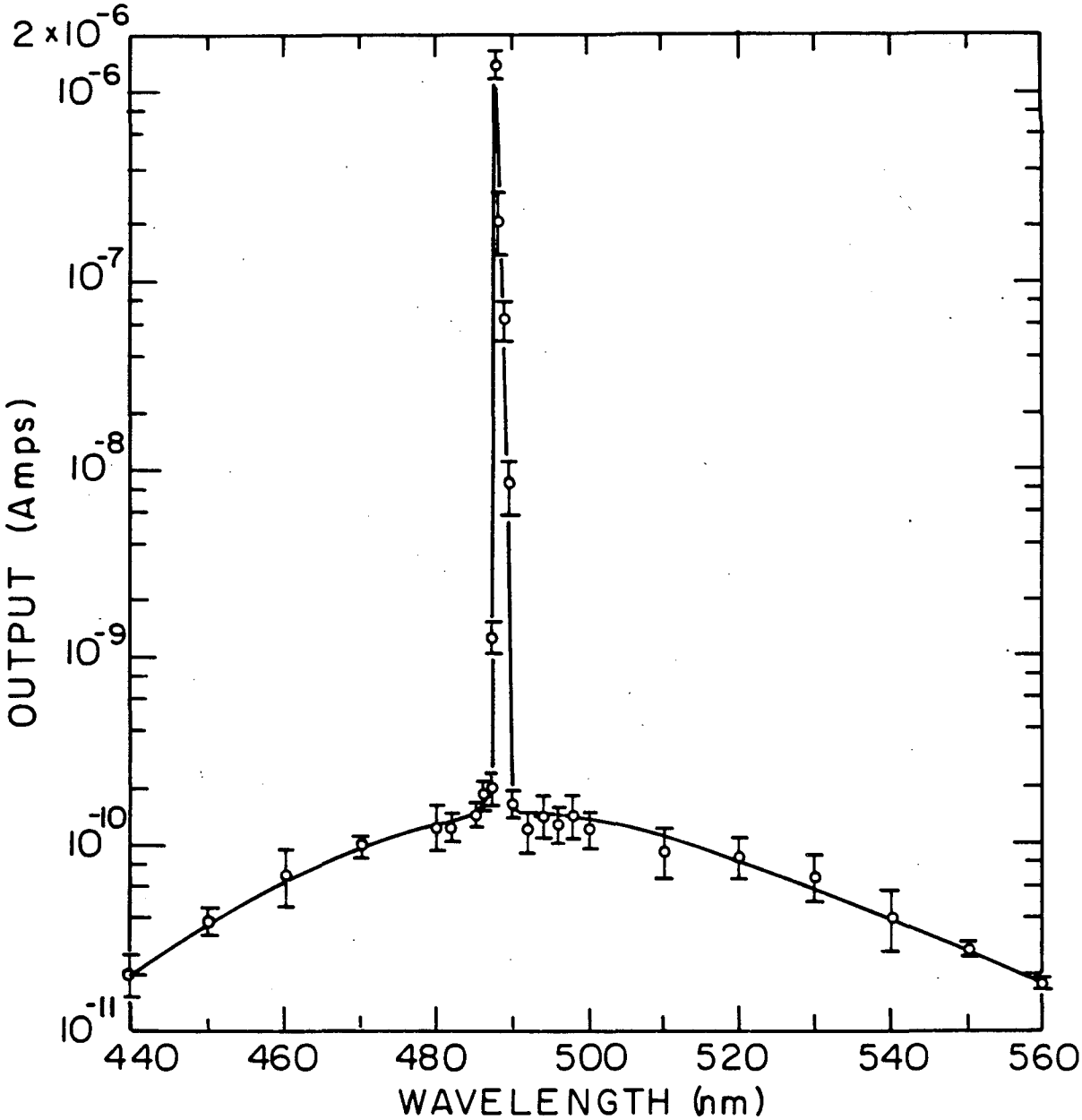

Fig. 2

XBL 805-5147

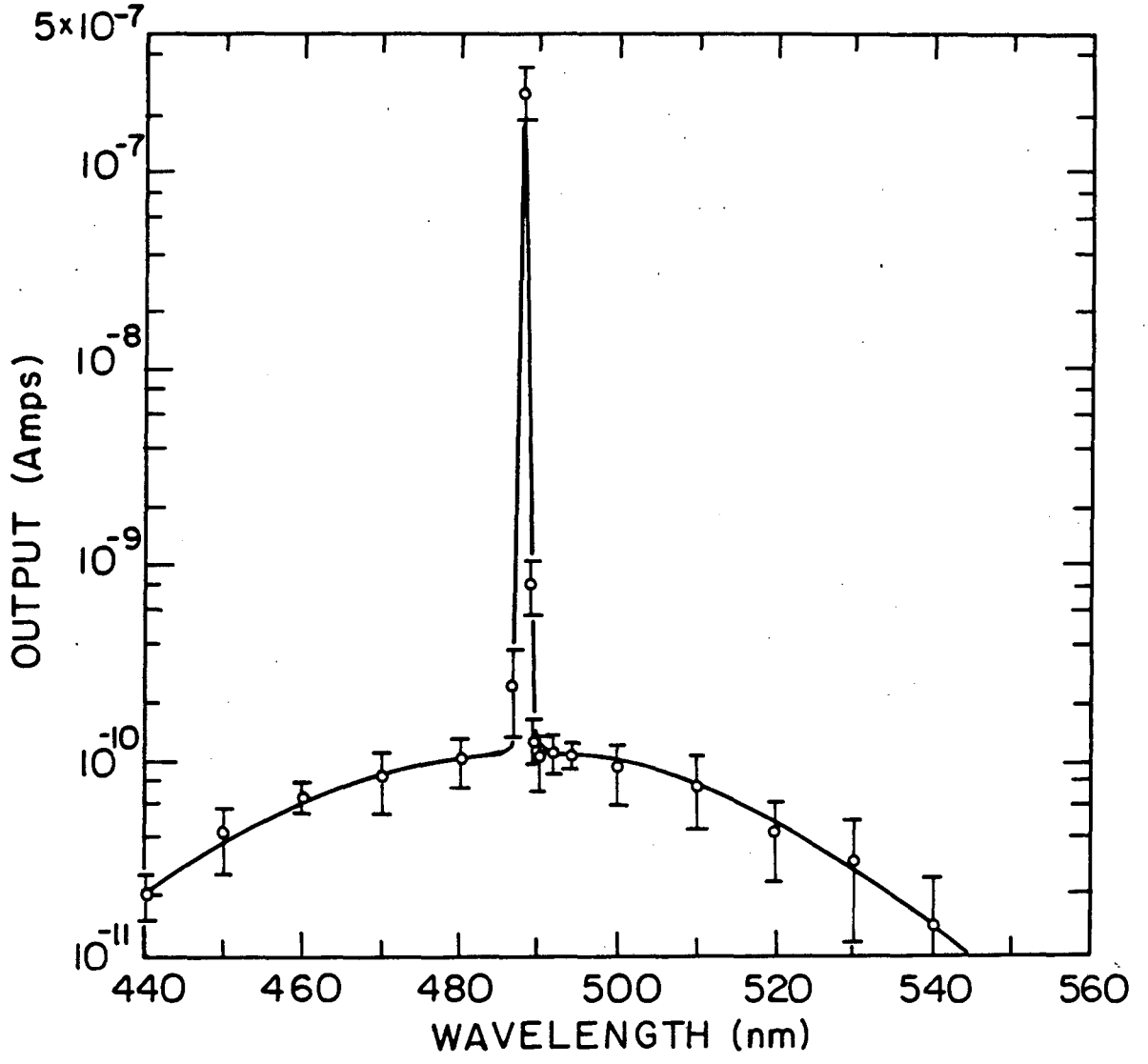

Fig. 3

XBL 805-5148

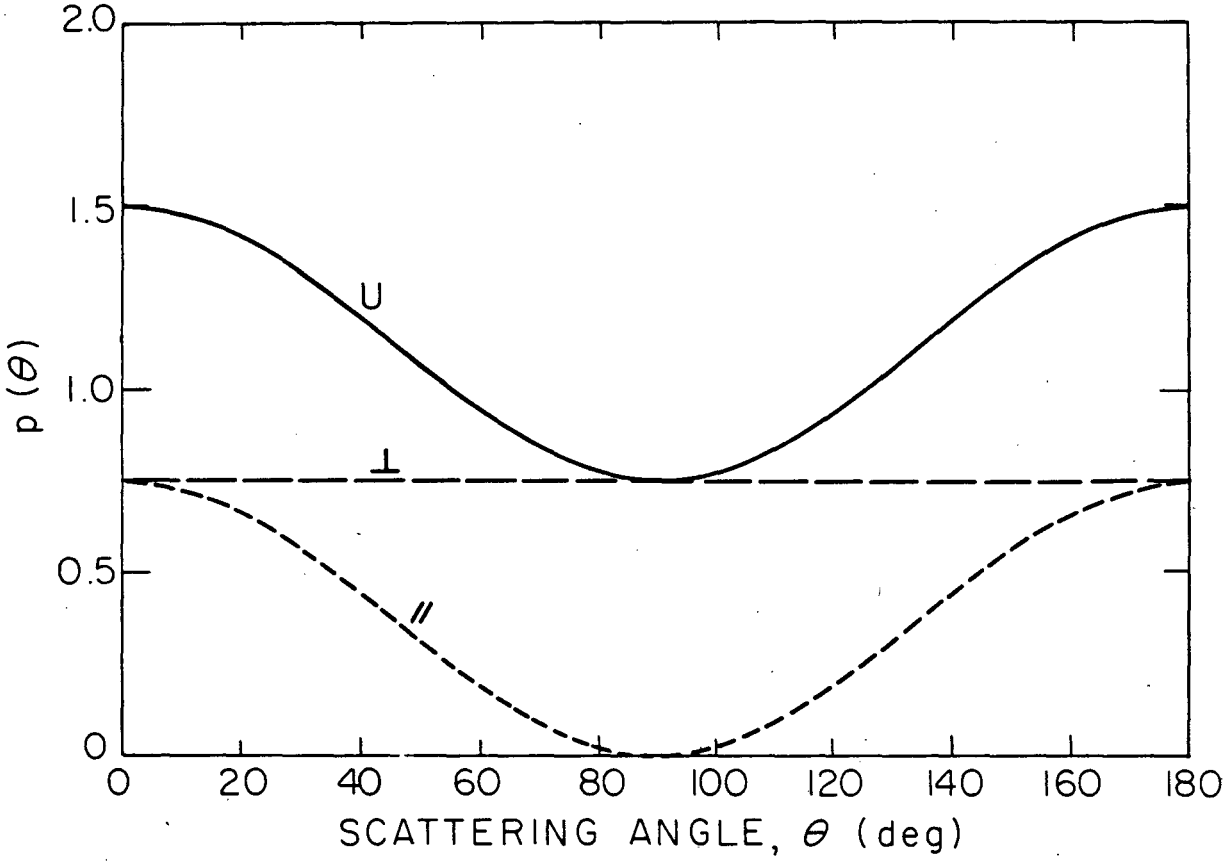

Fig. 4a

XBL805-5149

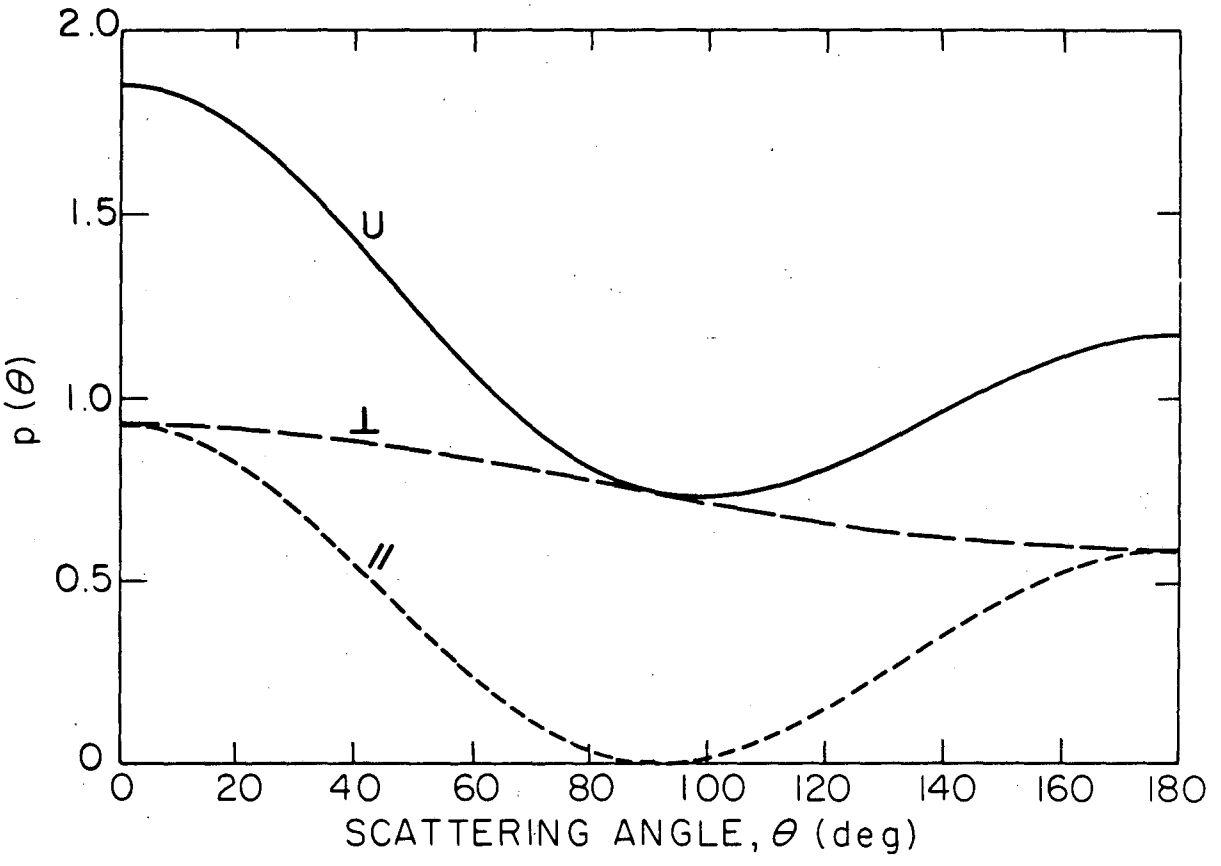

Fig. 4b

XBL 805-5150

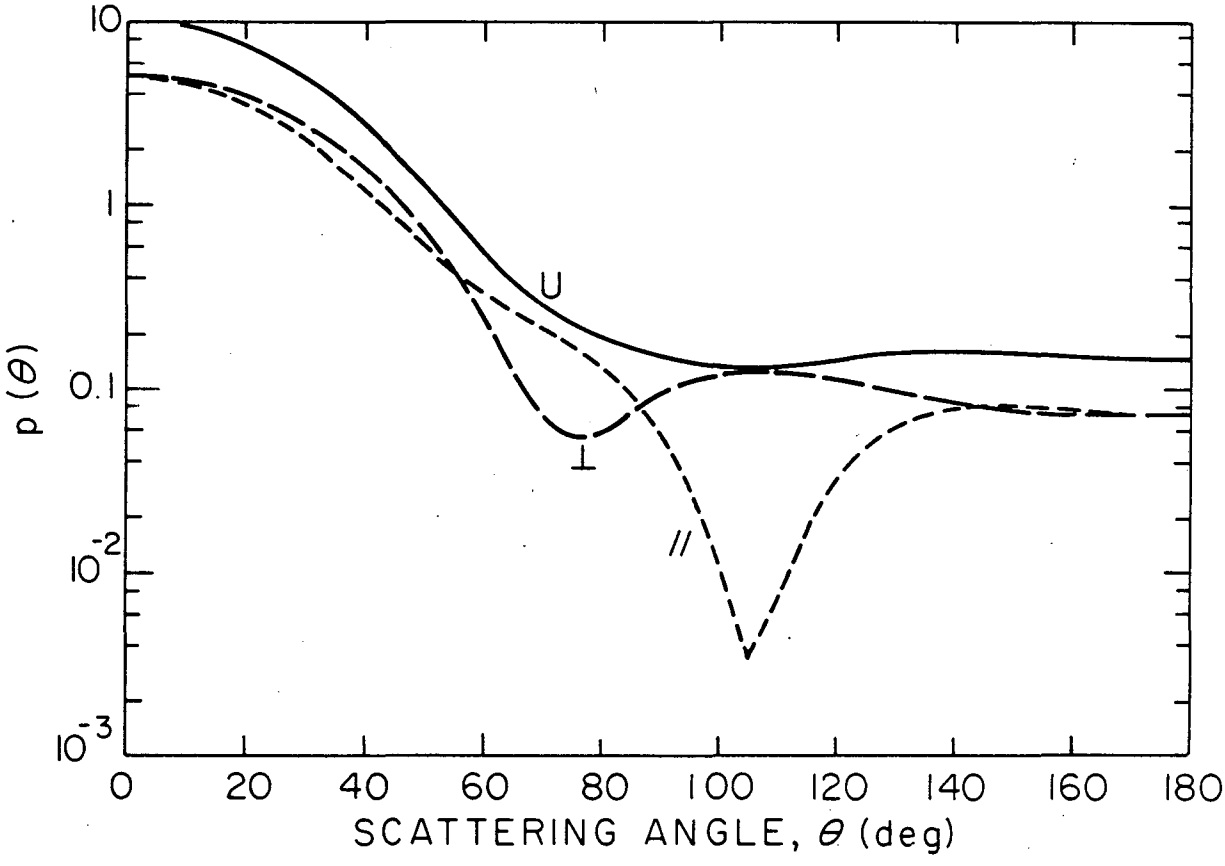

Fig. 4c

XBL805-5151

TECHNICAL INFORMATION DEPARTMENT
LAWRENCE BERKELEY LABORATORY
UNIVERSITY OF CALIFORNIA
BERKELEY, CALIFORNIA 94720